CHAPTER 24

# ACTIVE SEISMIC MONITORING OF THE SAN ANDREAS FAULT AT PARKFIELD

Valeri A. Korneev[a] *and* Robert M. Nadeau[b]

## Contents



## 1. INTRODUCTION

The town of Parkfield, located on the San Andreas Fault in central California has been the site of intensive multidisciplinary earthquake studies since the 1970s. Moderate-sized earthquakes of about magnitude 6 have occurred on the Parkfield section of the San Andreas Fault at fairly regular intervals—in 1857, 1881, 1901, 1922, 1934, and 1966. The 1857 event was a foreshock of the great Fort Tejon earthquake (magnitude 8(1/4)), which ruptured the fault from Parkfield to the southeast for over 180 miles. Available data suggest that all six moderate-sized Parkfield earthquakes may have been "characteristic," in the sense that they all ruptured at the same area on the fault. The goal of research in the Parkfield area has been to observe the fault and surrounding crust, at close range and at high resolution before, during, and after a large, damaging earthquake, so as to better understand the earthquake process and to provide a scientific basis for earthquake prediction and hazard assessment.

Recognizing this hazard and the regular periodicity of recurring events near Parkfield, the US Geological Survey and the State of California

[a] Lawrence Berkeley National Laboratory, Berkeley, California, USA
[b] University of California at Berkeley, Berkeley, California, USA

*Handbook of Geophysical Exploration: Seismic Exploration*, Volume 40 
ISSN 0950-1401, DOI: 10.1016/S0950-1401(10)04029-2

began a comprehensive, long-term Parkfield Earthquake Prediction Project, reported in Bakun and Lindh (1985). More than 100 researchers have been involved in various facets of this project. It was assumed that the next characteristic earthquake would nucleate in the same location as the 1966 event at Middle Mountain, northwest of Parkfield. This area, located at the beginning of the SAF creeping section, has a naturally high seismicity level. Middle Mountain, the central point of the area, is heavily instrumented with various geophysical sensors, including a High-Resolution Seismic Network (HRSN). However, the expected characteristic event occurred in 2004 and was nucleated in the middle of Cholame Valley, 22 km southeast of Parkfield, in the locked section of the SAF, rather far from the instrumented area.

## 2. HRSN

The HRSN (Figure 1) established at Parkfield, CA in 1987 records exceptionally high-quality data, owing to its 13 closely spaced three-component borehole sensors, its very broadband recordings (0-125 Hz), and its sensitivity (recording events below magnitude 0.5), (Karageorgi et al., 1992). Several aspects of the Parkfield region make it ideal for the study of seismic wave propagation and small earthquakes, and their relationships to tectonic processes. These include the fact that the network spans the expected nucleation region of a repeating Magnitude 6 event and the transition from locked to creeping behavior on the San Andreas fault, the availability of three-dimensional P and S velocity models, a complete seismicity catalogue, a well-defined and simple fault segment, and a homogeneous mode of seismic energy release, as indicated by the earthquake source mechanisms. More than 11,000 earthquakes have been recorded since 1987, in the magnitude range $-1 < M < 5$.

## 3. Vibroseis Monitoring

A unique data set of seismograms for 720 source-receiver paths was collected as part of a controlled source Vibroseis experiment. In the experiment, seismic waves repeatedly illuminated the epicentral region of the expected M6 event at Parkfield from June 1987 until November 1996. For this effort, a large shear-wave vibrator was interfaced with the three-component (3-C) borehole HRSN, providing precisely timed collection of data for detailed studies of changes in wave propagation associated with stress and strain accumulation in the fault zone. Data collected by the borehole network were examined for evidence of changes associated with the nucleation process of the anticipated M6 earthquake at Parkfield (Karageorgi et al., 1992, 1997). These investigations reported significant

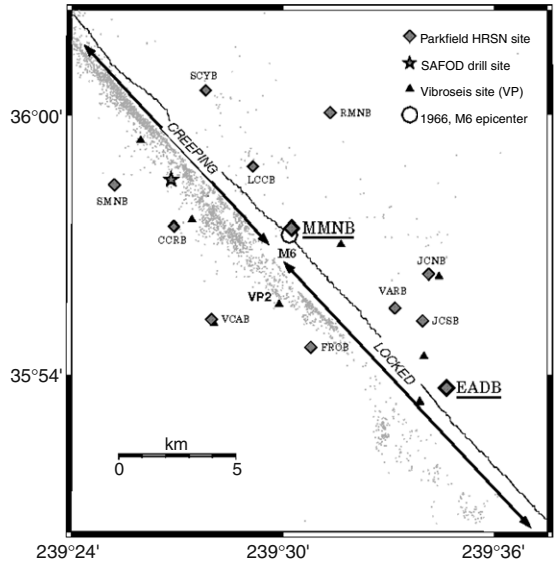


**Figure 1** Map showing the San Andreas Fault trace, and the location of the original 10 Parkfield HRSN stations. Relocated seismicity (1987 to mid-1998) is also shown, as are the locations of the 8 source points of the Vibroseis wave propagation monitoring experiment. The epicenter of the 1966 M6 Parkfield main shock and location of the San Andreas Fault Observatory at Depth (SAFOD) drill site are also shown.

travel-time changes in the S- coda for paths crossing the fault zone southeast of the epicenter and above the rupture zone of the 1966 M6 earthquake. Progressively decreasing travel times through the anomalous region changed by over 50 ms by the end of the study. Analysis and modeling of these data and comparison with observed changes in creep, water level, microseismicity, slip-at-depth, and propagation from characteristic repeating microearthquakes showed temporal variations in a variety of wave-propagation attributes—attributes that were synchronous with changes in deformation and local seismicity patterns (Karageorgi et al., 1992; Langbein et al., 1999; Roeloffs, 1998; Nadeau and McEvilly, 1999; Korneev et al., 2000).

The most important result of the Karageorgi et al. (1997, see their Figure 4), studies was the localization of the region of wave-propagation changes to the upper 3-4 km of the San Andreas Fault Zone, just above the locked zone of the expected M6 event. The creeping and seismically active northwestern part of the SAF showed no travel-time changes, while the most substantial changes were observed in the locked southeastern part of the Parkfield region of the SAF. It was hypothesized that these localized changes were in response to changing fluid conditions in the upper crust, induced by tectonic deformation, as well as stress and strain accumulation in the locked

section of the fault at depth. Additionally, Vibroseis VSP experiments in the nearby Varian well measured and monitored shear-wave anisotropy (Daley and McEvilly, 1990, 1991).

## 4. Origin of Changes

At Parkfield, the San Andreas Fault zone is a striking near-vertical low-velocity zone, and it very clearly acts as a waveguide for seismic energy from earthquakes on the fault and from surface sources. Velocity models there show a high Vp/Vs ratio along the fault, both near the surface and at depth, within the fault zone, and a pronounced vertical velocity gradient in the upper 2 km of the section (Michelini and McEvilly, 1991). The geometry of the Vibroseis source and receiver network, the approximate two-dimensionality of the fault zone in the region of the travel-time anomaly, and the existence of detailed P- and S-wave velocity models for the area all combine to provide well-determined constraints for modeling the observations. In Korneev et al. (2000), only data recorded at stations VCAB and JCNB from vibrator site VP2 were considered (Figure 1). At VP2, we have the routine Vibroseis monitoring data from the repeated point source, as well as a cross array of sources with 17 vibrational points at each leg.

The modeling exercise was confined to the VP2 data for VCAB and JCNB stations, for several reasons. Both source-receiver paths are in the anomalous region and reveal substantial travel-time variations. Moreover, the two paths are approximately co-linear and orthogonal to the San Andreas Fault, permitting the use of a two-dimensional formulation in simulating wave propagation. The path sample segments on the two sides of the fault zone have similar length. Finally, the data profile from the closely spaced source array at VP2 defines the spatial coherency of the wavefield, which is helpful in phase identification and interpretation of the recorded wavefield. The velocity model used in numerical simulation incorporates the known properties of the region, where tomographic three-dimensional velocity models have already been determined (Michelini and McEvilly, 1991). A major factor controlling the character of wave propagation at short range from a surface source is the severity of the shallow vertical velocity gradient. Values of velocity gradient in the model were determined by matching the observed and computed direct arrivals in the early part of the seismograms. For the NE side of the fault, the direct arrivals at JCNB could be matched with a velocity profile reduced by a factor 0.76 for that of VCAB, and by 0.5 for the narrow fault zone, modeled as a vertical layer with a thickness of 200 m. Computations were performed using a 2-D elastic finite-difference formulation. Two features dominated the process: energy trapping near the surface by the shallow gradient, and wavefield scattering from the fault zone. Most of the energy is confined to the upper part of the section in multiple

reflections at the free surface, producing a complex train of surface-guided waves made up of many arriving phases.

The signatures of the fault zone and shallow gradient on the wavefield are dramatic. In the interval between the first-arriving P and S waves at VCAB, surface-generated multiples and conversions take place. The latter are especially strong for P-waves, e.g., PS and PPS. Strong reflections are also produced by both fault-zone boundaries. At JCNB, the internal fault-zone reflections produce sequences of strong, distinct arrivals following the direct P and S waves. The times in the synthetic seismograms where large travel-time changes were observed in the monitoring project at VCAB and JCNB contain significant energy that has been reflected from the fault zone. This result suggests a ready explanation for the cause of the observed progressively decreasing travel-times: For the path VP2-VCAB, the changes were seen at arrival times after 3.5 s, after the direct waves have passed and the fault-zone reflected waves arrive. On the other hand, the travel-time changes for the VP2-JCNB fault-crossing path begin with the arrival of the direct P wave and occur through the entire seismogram. These results represent strong evidence that the observed variations are most likely caused by changes within the fault zone itself. Observed travel-time changes nicely fit the modeled results for seismograms computed for a 6% velocity increase localized in the narrow fault zone.

Three key conclusions follow from this study: (1) a strong subsurface velocity gradient is a key factor in wave propagation excited by surface-placed sources; (2) use of surface sources allows observations of waves reflected from the SAF and track changes in those waves; (3) observed changes originate in the locked part of the fault core. Unfortunately, the Vibroseis monitoring experiment was terminated in 1996, and the evolution of monitored changes up to the 2004 M6 Parkfield earthquake is unknown.

## 5. Guided-Wave Imaging of SAF Core

Observations and numerical models testify to the imaging power of fault zone guided waves (FZGW) to characterize, spatially and temporally, the properties and processes within the central cores of major active fault zones. Fault-zone guided waves were identified as such by Aki and co-workers in active-source, surface-to-borehole studies and later in seismograms recorded in or near the fault zone from local earthquakes (Leary et al., 1985; Li et al., 1990). These waves are most visible for sources within a well-developed fault zone and receivers located within the same fault zone segment (Li et al., 1994, 1997) although they appear also to be generated by off-fault surface sources (Korneev et al., 2000). The FZGW appear to be trapped by the presence of material in a fault that has a lower seismic wave velocity than the surrounding, more intact rock, from which it is separated by relatively sharp boundaries—the low-velocity nature of the

San Andreas Fault zone core has long been recognized (Feng and McEvilly, 1983). FZGW are seen in the codas of both the direct P and S waves, but they are usually much stronger in the S-wave coda, with large amplitudes in some cases arriving twice as late as the S-wave travel time (Karageorgi et al., 1997). They usually exhibit lower frequency than the direct P or S waves, and in many cases they appear to be dispersive.

There are compelling reasons to study the FZGW phenomenon. First, it has the potential for defining the structure of the active fault zone at depth. Second, the features that bound rupture extent in large earthquakes (segmentation boundaries, gaps, streaks, or asperities) may be evident in FZGW generation and propagation characteristics. Third and finally, the degree to which processes already under way in the cores of seismogenic fault zones can be detected and monitored is unknown—but is of critical importance in seismology. Detection of transient or systematic changes within the fault core through successful FZGW imaging in four dimensions is a potentially powerful monitoring method (Li et al., 1998; Ben-Zion et al., 2003). This is particularly true at Parkfield, where the San Andreas is a low-velocity zone striking near-vertically (Michelini and McEvilly, 1991) and clearly acting as a waveguide for seismic energy from earthquakes and surface sources (Li et al., 1998; Korneev et al., 2000). Velocity models also show a high Vp/Vs ratio along the fault near the surface and at depth within the fault zone, and a pronounced vertical velocity gradient in the upper 2 km of the section. The geometry of the Vibroseis source and receiver network, the approximate two-dimensionality of the fault zone in the region of the travel-time anomaly, and the existence of detailed P- and S-wave velocity models for the area all combine to provide well-determined constraints in modeling FZGW observations. Numerical modeling and microearthquake data indicate that FZGWs propagate within an SAF zone that is 100 to 200 m wide at seismogenic depths, and has a 20%–40% lower shear-wave velocity than the adjacent unfaulted media. The initial step in our FZGW investigation of the SAF was to look at the nature of FZGWs with respect to the hypocenter source location and receiver position, to map any obvious features in the spatial relationship of source and receiver. Two stations are close enough to the fault zone to provide a conveniently "reversed" profile of sources along the fault (by building "station gathers" of traces).

Results from Korneev et al. (2003) confirm that FZGW at Parkfield are generated within the fault zone and are most prominent late in the coda of S, while also seen in the P coda. Also, FZGW amplitude inversion enables vertical section imaging of the delineation zone between creeping and locked parts of SAF. Most likely, the variation in FZGW attenuation is associated with fracture closure and opening, caused by the evolution of stress-induced changes in loading. Laboratory measurements of time-lapse seismic attenuation in fractured rock under increasing normal load show an initial steady increase in Q (due to closure of preexisting micro-fractures in the rock) that reaches a maximum value plateau, and then decreases rapidly

(due to the formation of new fractures) just prior to catastrophic failure of the rock (Sobolev et al., 1996).

The spatial distribution of Q at Parkfield indicates that a similar process may be occurring within the zone of concentrated stress buildup and release associated with magnitude 4 and 5 earthquakes. The process of fracture closure and opening is also expected to involve dewatering and saturation of rocks (respectively), and corresponding changes in water pressure, all of which are expected to result in seismic propagation variations. We interpret the localized zone of FZGW low attenuation as the NW edge of the M6 asperity at Parkfield, at the transition of the SAF locked and creeping behavior at depth, with the high Q, due most likely to dewatering resulting from fracture closure and/or fault-normal compression. A greater understanding of the relationships between FZGW attenuation, and stress-related fracturing processes under conditions of accumulating fault stress, will be needed to obtain information useful for understanding the earthquake nucleation process and for possibly predicting earthquakes.

A particular strength of using FZGWs to study the detailed structure and deformation of an active fault zone is that FZGW propagation is confined to the fault core, making them highly sensitive to any spatial or temporal variations along the fault. In contrast, the propagation paths of direct P- and S-waves from earthquakes occurring within the low-velocity fault zone take place largely outside of the fault core in the higher-velocity country rock. As a result, direct P- and S- arrivals contain little information on the properties of the fault itself. This limits the resolution on fault structure that direct P- and S-waves can provide to about 5 km. In contrast, we have already shown that FZGWs can resolve the details of fault structure on the order of 50 m (Korneev et al., 2000).

By increasing the number of receiver stations located directly on the fault, it should be possible to improve resolution even further. Analysis of seismograms from a cluster of 12 microearthquakes exhibit practically identical waveforms, although the magnitudes of the events belonging to that cluster clearly show strong temporal variations (Figure 2). The ray paths of this cluster intersect the FZ attenuation anomaly, which was found by tomographic inversion. Cross-correlation of the cluster waveforms reveal no travel-time changes for all recorded phases, including direct P, S, and guided waves. In contrast, amplitudes of guided waves show strong changes compared to P- and S-wave amplitudes. These changes correlate spatially and temporally with overall Parkfield seismicity, suggesting their common origin (Korneev and Nadeau, 2004).

The previous studies showed the potential of FZGW for imaging and monitoring the inner part of the FZ. However, only waves generated by natural seismicity were used there, and as a result, the creeping part of the fault comprised most of the fault image. Note that use of active sources would enable seismologists to study the locked part of the SAF, reaching the areas where the actual 2004 M6 Parkfield earthquake originated.

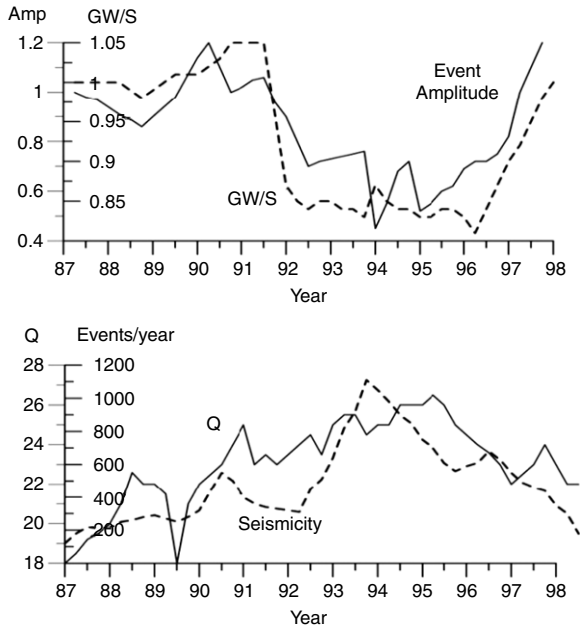


**Figure 2** Observed changes during the years 1987-1999 in Parkfield, California. Upper panel shows the amplitude of repeating cluster events (solid line) and amplitude ratio of GW to S waves for the same events (dashed line). Lower panel shows evolution of Q at the cluster hypocenter (solid line) computed using attenuation tomography (Korneev et al., 2003), and year-average seismicity in Parkfield area (dashed line). Guided wave amplitude changes are the most pronounced, whereas no detectable changes were found in body wave travel.

## 6. Fault Continuity Testing

The continuity of low-velocity layers is a very important problem in geophysics. Promising results from exploration geophysics demonstrate the ability of guided waves to propagate in low-velocity sedimentary layers at distances substantially exceeding those of regular body waves (Korneev and Myer, 2001; Parra et al., 2001).

The detailed studies of seismicity generated by the 1966 Parkfield M6 event revealed very high seismic activity in the Cholame Valley region southeast of Parkfield, as well as ruptures along the Cholame Valley tracing the fault along the surface. In the middle of the valley, the SAF had about a 1.5 km jog to the southwest, after which it continued southeast, staying parallel to the original direction. The jog geometry had no surface evidence and was determined on the basis of epicenter locations for multiple events in this area. Seismic and theoretical studies (Hanna et al., 1972; Eaton et al., 1970) suggest the complex structure of the jog area, with

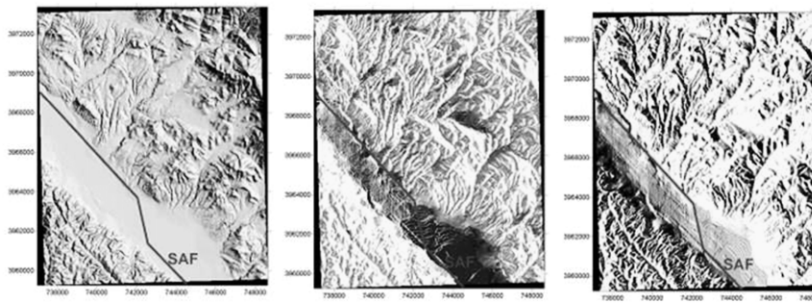


**Figure 3** Steep-angle light imaging reveals details of the small-scale topography in the Cholame Valley, which suggests the existence of a fault echelon between SAF strands. Solid line indicates the current mapping of the SAF trace.

interacting segments of two parts of the SAF. Such segments usually represent wide zones, with multiple fractures oriented at 45° with respect to the main fault orientation, and which connect isolated segments of a fault. The corresponding microfracturing was observed in multiple locations of Cholame Valley. The extent and mechanical properties of interacting segments have a strong impact on accumulated strain release.

The importance of this SAF element lies in the fact that this jog was the originating point of the 2004 Parkfield earthquake. The fault-structure studies in Cholame Valley are mostly based on seismic information, because valley sediments cover bedrock and do not allow accurate fault mapping. Nevertheless, we have found that low-amplitude topography features of the valley are apparently affected by bedrock surface geometry. We subsequently analyzed shade relief images by varying color saturations and light-source positions. The shade relief technique has spatial differentiating properties and enables delineation (Figure 3) of both delicate and pronounced topographic details. An existing proposed point of jog connection with the southwest strand of the SAF is observed; the fault can be traced along both sides through this point. Multiple NS-oriented faults that make 45° angles with traces of the SAF are quite visible. Image features also suggest a straight continuation of the NW part of the SAF in the SE direction after passing the jog. At the same time, the NW straight extension of the SE part of the SAF connects it with mapped parts of the South-West Fracture Zone (SWFZ), which extends quasi-parallel to the SAF.

This result suggests that the Cholame Valley fault structure represents two faults separated at some point in time, but which began interacting through the development of shear-faulting in the middle of the valley, leaving some of their old parts temporarily inactive. This hypothesis can be tested using fault-zone guided waves, since inactive faults still should have low-velocity properties, owing to the relatively high concentration of fractures within the zones. A corresponding experiment should include excitation of

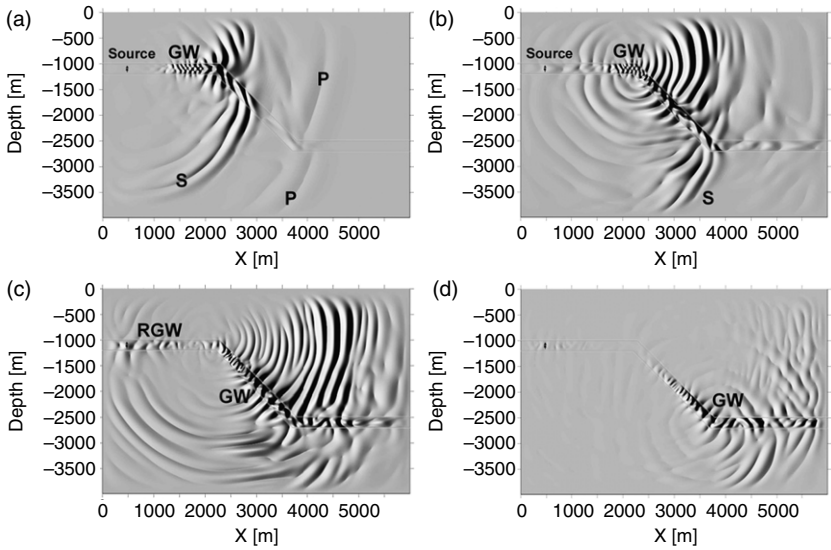


**Figure 4** Consecutive snapshots for the SAF jog model. Note the reflected guided waves (RGW) in panel (c), as well as the strong emission of S-wave energy coming from bends. Despite the complex geometry, the GW energy is well trapped in the FZ.

fault-zone guided waves by placing explosive and/or vibroseismic sources on a known existing fault zone (in particular on SWFZ), with surface-seismic-line recording across the anticipated trace of this fault at a 5-10 km distance from the source. Detection of FZGW should indicate the continuity of low-velocity properties along the source-receiver path to support the suggested model of fault structure.

We performed a 2-D numerical experiment to study guided-wave propagation along a jog-shaped waveguide. A finite-difference method with a staggered grid was used for modeling. The embedding medium has wave propagation velocities of Vp = 4000 m/s, Vs = 2.4 m/s, and a density of 2.7 g/cm$^3$, containing a 200 m wide waveguide with geometry as shown in Figure 4. A vertical-force source was placed in the middle of the waveguide (Figure 4(a)). Panels in Figure 4 represent four consecutive snapshots for field amplitudes as waves propagate in and out of the FZ.

Several interesting effects are shown by this experiment. First, 45° sharp bends keep most of the energy inside of the waveguide. Second, these bends generate visible reflected guided waves (RGW) that propagate backwards, indicating discontinuities in fault properties. Third, the turning direction of guide-wave propagation occurs at the expense of increased S body-wave radiation in the outer medium. The directions of wave propagation are close to the initial propagation direction of the guided waves, as if wave energy exhibits an "inertial" influence (Figure 4(c)). These

effects suggest additional potential utilization of guided-wave energy for FZ characterization purposes. For seismology, knowledge of a fault's structure and composition has critical significance for the modeling and prediction of future earthquake scenarios.

## 7. Discussion and Conclusions

The lack of natural seismic events around the nucleation zone of the 2004 M6 Parkfield earthquake stresses the importance of active controllable seismic monitoring in the zones of potential earthquakes. Monitoring changes associated with processes in the core of the fault zone should provide valuable information about fault conditions and potentially lead to a better understanding of strong earthquakes. Use of a controlled source for guided wave monitoring is most desirable, since with a controlled source, the exact source location and initiation time are known. Explosion sources are not highly repeatable and require special permissions and precautions. A conventional Vibroseis source cannot be used for FZGW monitoring, since its lowest excitation frequency is around 8 Hz, whereas FZGW energy is in the 3-6 Hz band. On the other hand, low-frequency eccentric vibrators (LEV) would be an ideal source for fault zone monitoring using guided waves (Alexeev et al., 2005). With modern modeling techniques, FZGWs can provide detailed images of a fault zone's inner structure and other characteristics. Placing an active, low-frequency source on top of an FZ core and a line of surface receivers intersecting the FZ behind a potential nucleation zone, we can achieve an FZGW monitoring scheme (Figure 5).

In a complementary active monitoring scheme, sources can be placed far outside of the FZ and illuminate a large (10-30 km) FZ area containing a potential nucleation zone. A specially placed line of seismometers can record the waves that intersect the FZ at seismogenic depths. Changes in FZ properties under stress-strain variations will cause corresponding changes in waves transmitted through the FZ and can be interpreted after detection. For this scheme, the use of an ACROSS source (Kunimoto and Kumazawa, 2004) seems the most appropriate, because of its high durability and precision. This scheme is also shown on Figure 5.

Parkfield is an ideal location for active monitoring experiments because of: (1) the number of ongoing important experiments in the area, (2) its high earthquake hazard, (3) its relatively regular earthquake-recurrence interval, and (4) its long-term baseline of monitoring results for various geophysical observables. Understanding the detailed structure, physical properties, and evolution of the fault at depth is critical to advancing our knowledge of earthquake physics, formulating estimates of earthquake hazards, and developing schemes for hazard reduction. FZGW studies show promise for identifying blind faults and fault continuity across

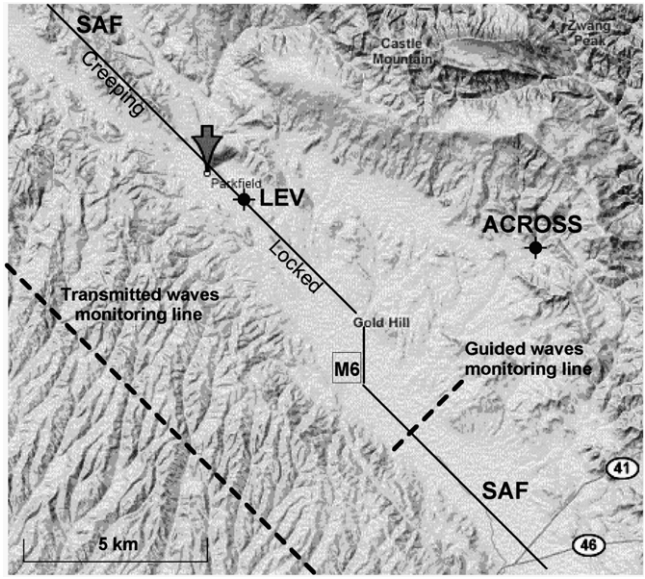


**Figure 5** Conceptual SAF active monitoring scheme in the Cholame Valley. The LEV source excites low-frequency GW, which propagate along the SAF to be recorded by the GW monitoring line. Waves excited by the ACROSS source transmit through the SAF at seismogenic depths to be recorded by a transmitted-waves monitoring line. The square indicates the epicenter of the 2004 M6 event.

jogs and at depth. Deep-well seismometers installed during the SAFOD (http://earthquake.usgs.gov/research/parkfield/safod_pbo.php) project also present a major opportunity for controlled source experiments in the Parkfield area.

## Acknowledgments

Data processing was done at the Center for Computational Seismology (CCS) at LBNL, which is operated by the University of California for the US Department of Energy (DOE) under Contract No. DE-AC03-76SF00098. The USGS provided financial support for this research through NEHRP Award 1434-95-G-2540, and support for the Berkeley Seismological Laboratory's operation of the HRSN is through Grant No. 07HQAG0014.

## *REFERENCES*

Alexeev, A.S., Chichinin, I.S., Korneev, V.A., 2005. Powerful low-frequency vibrators for active seismology. Bulletin of the Seismological Society of America 95 (1), 1–17.

Bakun, W.H., Lindh, A.G., 1985. The Parkfield, California, prediction experiment. Earthquake Prediction Research 3, 285–304.

Ben-Zion, Y., Peng, Z., Okaya, D., Seeber, L., Armbruster, J.G., Ozer, N., Michael, A.J., Baris, S., Aktar, M., 2003. A shallow fault-zone structure illuminated by trapped waves in the Karadere-Duzce branch of the North Anatolian Fault, western Turkey. Geophysical Journal International 152, 699–717.

Daley, T.M., McEvilly, T.V., 1991. Update of shear-wave anisotropy measurements at the Parkfield Varian well. Seismological Society of America, Annual Meeting.

Daley, T.M., McEvilly, T.V., 1990. Shear-wave anisotropy in the Parkfield Varian Well. Bulletin of the Seismological Society of America 80, 857–869.

Eaton, J.P., O'Neill, M.E., Murdock, J.N., 1970. Aftershocks of 1966 Parkfield-Cholame, California Earthquake: A detailed study. Bulletin of the Seismological Society of America 60 (4), 1151–1197.

Feng, R., McEvilly, T.V., 1983. Interpretation of seismic reflection profiling data for the structure of the San Andreas Fault zone. Bulletin of the Seismological Society of America 73, 1701–1720.

Hanna, W.F., Burch, S.H., Diblee, T.W., 1972. Gravity, magnetics, and geology of the San Andreas fault near Cholame, California, US Geological Survey Professional Paper 646-C.

Karageorgi, E., Clymer, R., McEvilly, T.V., 1992. Seismological studies at Parkfield: II. Search for temporal variations in wave propagation using VibroseisVibroseis. Bulletin of the Seismological Society of America 82, 1388–1415.

Karageorgi, E.D., McEvilly, T.V., Clymer, R.W., 1997. Seismological studies at Parkfield IV: Variations incontrolled-source waveform parameters and their correlation with seismic activity 1987–1994. Bulletin of the Seismological Society of America 87 (1), 39–49.

Korneev, V.A., Myer, L.R., 2001. Testing of sedimentary layer continuity using guided waves. Gas Research Institute Topical Report.

Korneev, V., Nadeau, R., 2004. Vibroseis monitoring of San Andreas Fault in California. In: Proceedings Paper for the International Workshop in Active Monitoring. Mizinami, Japan, pp. 88–95.

Korneev, V.A., Nadeau, R.M., McEvilly, T.V., 2003. Seismological studies at Parkfield IX: Fault zone imaging using guided wave attenuation. Bulletin of the Seismological Society of America 93 (4), 1415–1426.

Korneev, V.A., McEvilly, T.V., Karageorgi, E.D., 2000. Seismological studies at Parkfield VIII: Modeling the observed travel-time changes. Bulletin of the Seismological Society of America 90 (3), 702–708.

Kunimoto, T., Kumazawa, M., 2004. Active monitoring of the earth's structure by seismic ACROSS. In: 1st International Workshop on Active Monitoring in the Solid Earth Geophysics. Mizunami, Japan, pp. 181–184.

Langbein, J., Gwyther, R., Hart, R., Gladwin, M.T., 1999. Slip rate increase at Parkfield in 1993 detected by high-precision EDM and borehole tensor strain meters. Geophysical Research Letters 26, 2529–2532.

Leary, P.C., Li, Y.-G., Aki, K., 1985. Borehole observations of fault zone trapped waves, Oroville, CA. Transaction EOS 66, 976.

Li, Y.-G., Ellsworth, W.L., Thurber, C.H., Malin, P.E., Aki, K., 1997. Fault-zone guided waves from explosions in the San Andreas fault at Parkfield and Cienega Valley, California. Bulletin of the Seismological Society of America 87, 210–221.

Li, Y.-G., Leary, P.C., Aki, K., Malin, P.E., 1990. Seismic trapped modes in the Oroville and San Andreas fault zones. Science 249, 763–766.

Li, Y.-G., Vidale, J.E., Aki, K., Marone, C., Lee, W.H.K., 1994. Fine structure of the Landers fault zone: Segmentation and the rupture process. Science 265, 367–370.

Li, Y.-G., Vidale, J.E., Aki, K., Xu, F., Burdette, T., 1998. Evidence of shallow fault zone strengthening after the 1992 M7.5 Landers, CA, earthquake. Science 279, 217–219.

Michelini, A., McEvilly, T.V., 1991. Seismological studies at Parkfield: I. Simultaneous inversion for velocity structure and hypocenters using B-splines parameterization. Bulletin of the Seismological Society of America 81, 524–552.
Nadeau, R.M., McEvilly, T.V., 1999. Fault slip rates at depth from recurrence intervals of repeating microearthquakes. Science 285, 718–721.
Parra, J.O., Hackert, C., Gorogy, A., Korneev, V.A., 2001. Detection of guided waves between gas wells for reservoir characterization, LBNL-48523. Geophysics 67 (1), 38–49.
Roeloffs, E., 1998. Persistent water level changes in a well near Parkfield, California, due to local and distant earthquakes. Journal of Geophysical Research 103 (B1), 869–889.
Sobolev, G.A., Babichev, O.V., Los, V.F., Kol'tsov, A.V., Ponomaryov, A.V., Ponyatovskaya, V.I., Rozanov, A.S., Stanchits, S.A., Khromov, A.A., Frolov, D.I., Yangquan, L., Jialiu, Z., Jiadong, Q., Shiyu, L., 1996. Precursors of the destruction of water containing blocks of rock. Journal of Earthquake Prediction Research 5.

Korneev, V. and R. Nadeau, 2010, Vibroseis Monitoring of San Andreas Fault in California: in Active Geophysical Monitoring, Handbook of Geophysical Exploration, Vol. 40, Elsevier, 449-462.

Vol. 40, Elsevier, 449-462.